Research Article

Qingyu Li, Laiyi Jing, Qunying Sun, Li Ji*, and Songying Chen*

The finite element modeling of the impacting process of hard particles on pump components

https://doi.org/10.1515/phys-2022-0048
received September 29, 2021; accepted April 25, 2022

Abstract: Shield pumps which transport a variety of complex media are widely used in chemical industry, mineral industry, and other fields. However, the hard particles in the media erode the flow passage in the shield pump, seriously affecting the service life of the pump. Therefore, it is important to study the erosion process in the flow passage to extend the service life of the pump. This erosion process in the shield pump can be investigated by experiments, but it is difficult for the current experimental method to copy the real industrial service environment of impellers. For example, the environment temperature and speed range are found difficult to be reached by the current experimental method. Comparatively, the simulation by finite element method can overcome the above deficiency. In this article, the ANASYS software is used to simulate the erosion process in shield pump flow passage due to hard particles. Specifically, the structural static analysis module is used to build the model of thermal barrier coating components and hard particle components. Then the variation law of stress, strain, and material deformation of the flow passage components under concentrated force is obtained. Second, the extended finite element method is used to study the crack propagation caused by the erosion process. A linear elastic–linear softening constitutive model is established to simulate the stress variation during the crack propagation and material removal under the continuous erosion from hard particles. The proposed law regarding stress variation and crack propagation in the erosion process in this study contributes to theoretical support for damage detection and service life extension of shield pumps.

Keywords: finite element method, hard particles, shielded pump, flow passage components, erosion wear, crack propagation

1 Introduction

The shield pump belongs to the non-sealed pump integrated with motor and pump. It uses the fluid medium as circulating liquid to cool the motor and lubricate the bearing. It is widely used in various industrial production because it has no leakage [1]. Shielding pumps are affected by the nature of the fluid being transported, fluid flow conditions, pump production parameters, production quality, *etc*. [2], which includes fluid density, impurity particle size, impurity particle hardness, impurity particle shape, fluid velocity, impact angle, and geometry and material of pumps. The materials transported by the shielding pump consist of two parts, *i.e*., hard particles and fluid. Therefore, the properties of hard particles and fluid–hard particles mixture collectively decide the material properties in the shield pump. According to the wear theory, the fluid drives the hard impurities to quickly impact the surface of the blade or pump to cause scouring, called as the impurity erosion. When the impinging impurities are trapped in the gas, jet erosion happens. Actually, the erosion of the shield pump is mainly due to the impurity erosion. The hard particles in the shield pump erode the material of the flow passage components, causing severe erosion wear [3,4].

Understanding erosion mechanism of the fluid medium on the material surface is helpful for mastering the erosion process and choosing suitable anti-erosion technology in

* **Corresponding author: Li Ji,** Key Laboratory of High Efficiency and Clean Mechanical Manufacture, Ministry of Education, School of Mechanical Engineering, Shandong University, Jinan, Shandong 250061, China, e-mail: liji@sdu.edu.cn
* **Corresponding author: Songying Chen,** Key Laboratory of High Efficiency and Clean Mechanical Manufacture, Ministry of Education, School of Mechanical Engineering, Shandong University, Jinan, Shandong 250061, China, e-mail: chensy66@sdu.edu.cn
Qingyu Li: Key Laboratory of High Efficiency and Clean Mechanical Manufacture, Ministry of Education, School of Mechanical Engineering, Shandong University, Jinan, Shandong 250061, China, e-mail: qingyu.li@mail.sdu.edu.cn
Laiyi Jing: Technical Center, Shandong Hualuhengsheng Chemical Co., Ltd., Dezhou, Shandong 253000, China, e-mail: 13326262312@163.com
Qunying Sun: School of Agriculture and Animal Husbandry Engineering and Intelligent, Shandong Vocational Animal Science and Veterinary College, Weifang, Shandong 261071, China, e-mail: sunqunying@126.com

the production. In recent years, a large number of scholars have carried out related research on the surface erosion mechanism of materials [5]. Finnie [6] established a plowing mechanism for tough materials to withstand hard particle impurities in non-orthogonal shots. Walker *et al.* [7] found the effect of solid particle size and flow rate on erosion wear of slurry pump impellers. Yimin [8] studied the variation of erosion wear characteristics of resin-based composites with particle volume fraction. And he discussed the wear mechanism in combination with the morphology of the wear surface. Kai [9] researched the wear mechanism and distribution law of the impeller of the flow element. The feasibility of the ceramic coating to protect and repair the impeller wear was also verified in this research. For the erosion mechanism, the theory proposed by Bahadir has been widely recognized [4]. The theory held that the erosion process is a complex process which combines both material removal and material deformation. Material removal means that the hard particles take the pump material away in the form of impact and forms an erosion defect. Material deformation means that the hard particles also cause damage to the pump material in the form of impact. The difference between them is that the pump material only undergoes plastic deformation after impact, forming voids. Actually, the deformation of the material around the void also causes damage to the pump material. The continuous impact of the hard particles on the pump material initiates at the deformation place. After further exertion of impact, the microcracks form on the pump surface and expand. The study [5] combing industrial application and theory shows that different geometries of shielding pump and different processing parameters obviously affect the erosion and wear process.

The parts of shield pumps that are in direct contact with the solid and liquid phases are called as the pump flow passage components. The material properties and surface quality of the flow passage component determine the performance of the fluid flowing in the shield pump. Material properties include traditional parameters, such as material strength, hardness, and plasticity. Because flow passage components are often impacted by hard particles in the fluid, the wear resistance of the flow passage components is extremely important. Normally, the materials with higher hardness have stronger wear resistance. Some scholars [2,3] found that the wear resistance should be a combination of plasticity and hardness. Differently with material properties, the surface quality of the components is mainly affected by the processing technology during the processing. Therefore, the high-precision machined surface can reduce the loss of flow passage components to a certain extent.

The impacting process of the hard particle on pump flow passage components is extremely complicated. During the impacting process, the flow path of the hard particles, the impact degree on pump parts, and the displacement of the inner wall of the pump parts after impact are the key conditions to determine the loss of the pump. In the experimental research, high-speed photography and particle image velocimetry are mainly used to study the impacting process of the hard particle on pump components. However, the experiments are expensive and time-consuming [10]. Lei *et al.* [11] used particle velocimetry to measure the velocity of solid particles in the pump, but he did not accurately obtain the impacted condition of the pump's inner wall. Due to the limitation in research methods and experimental conditions, the studies on the erosion and wear impact of hard particles on the flow wall surface and its contributory factors are quite limited. Therefore, there are no sufficient research results to be used to guide the anti-wear optimization design of the flow passage components in the slurry pump. With the development of computer technology, the finite element method has become an effective method to study erosion process due to the flexibility in setting load conditions and geometric parameters of calculation object [12–14].

Honghong [13] used ANSYS/LS-DYNA software to study the erosion resistance of the coating, and he also reported the erosion mechanics law of plastic materials and brittle materials. Li [15] employed the numerical method to predict and analyze the impact wear of the pipeline elbow. Zhongdong *et al.* [16] adopted the CFD full-flow channel numerical method to analyze the effect of different sediment concentration and particle size on the wear of centrifugal pump flow components. Shen [17]. simulated the solid volume fraction distribution in the impeller of the vane-type slurry pump and analyzed the movement law of solid phases. In summary, the research studies of numerical simulation on impact and collision mainly focus on the impacting resistance of steel structures and the solid phase movement in the pump. However, there are few numerical simulation studies on the erosion wear and crack propagation of pump flow passage components. Consequently, comprehensive theoretical understanding is absent.

In this article, the finite element method is used to simulate both the impacting process of the hard particles on pump and crack propagation of impeller materials. Correspondingly, the effects of impact velocity and impact angle of the hard particles on the impeller, and stress variation law both during crack growth and material removal under continuous impact of hard particles, are investigated.

This article is supposed to provide theoretical support for industrial applications.

2 Methods

In this section, the Structural Static Analysis module in ANSYS software is used to numerically simulate the impacting process of the hard particles on the flow passage components in the pump. Then, the variation law of stress, strain, and material deformation of the flow passage components under concentrated force is obtained. The impacting process of brittle material on blades is a variation process, which involves nonlinear numerical problems. The computation of this impacting process is extremely complex, especially for the problem of crack propagation. Therefore, in this section, a reasonable impeller blade model composed of multi-layer rectangular coating and interstitial filler is established. The specific structure is shown in Figure 1. Then the stress field is analyzed and the crack propagation in this process is studied.

2.1 Finite element modeling of impact process

For the modeling of impeller blade materials coated with thermal barrier, first, thermal barrier coating (TBC) components and hard particle are established with rectangular parallelepiped structure, based on the electron beam physical vapor deposition (EB-PVD) cuboid structure. TBC components are based on the industrial process and the layers are separated by low-density materials. Harrington alloy 276 (HAC276) is used for TBC.

The material properties of the blade coating are shown in Table 1 and Figure 1(a). The width of interstitial material g is 0.1 μm. The density of the interstitial material is 295 kg/m^3, the Young's modulus is 2 GPa, and the Poisson's ratio is 0.1. The hard particle is a rigid sphere with a radius of 25 μm and a density of 2,000 kg/m^3. Finally, the parts defined with different material properties are assembled. The horizontal axis is the x-axis and the vertical axis is the y-axis. The grid uses a four-node plane strain element (CPE4R) with a grid number of 26,000. In order to obtain more accurate simulation, the mesh is refined in the area where the hard particle is in close contact with the TBC as shown in Figure 1(b). The minimum mesh quality is 0.2764, and the average mesh quality is 0.971. It is also shown that the encrypted mesh quality meets the computational requirements. The initial boundary conditions are u_1 (the velocity of hard particle) = u_2 (the velocity of coating) = 0 at the bottom of the TBC.

In order to ensure the accuracy of the calculation, the process of impacting hard particles on the blade coating is checked by the grid independent study. The results are shown in Table 2. The maximum principal stress decreases with the increase in the number of grids. We use the difference of the maximum principal stress corresponding to the number of adjacent grids as the criterion.

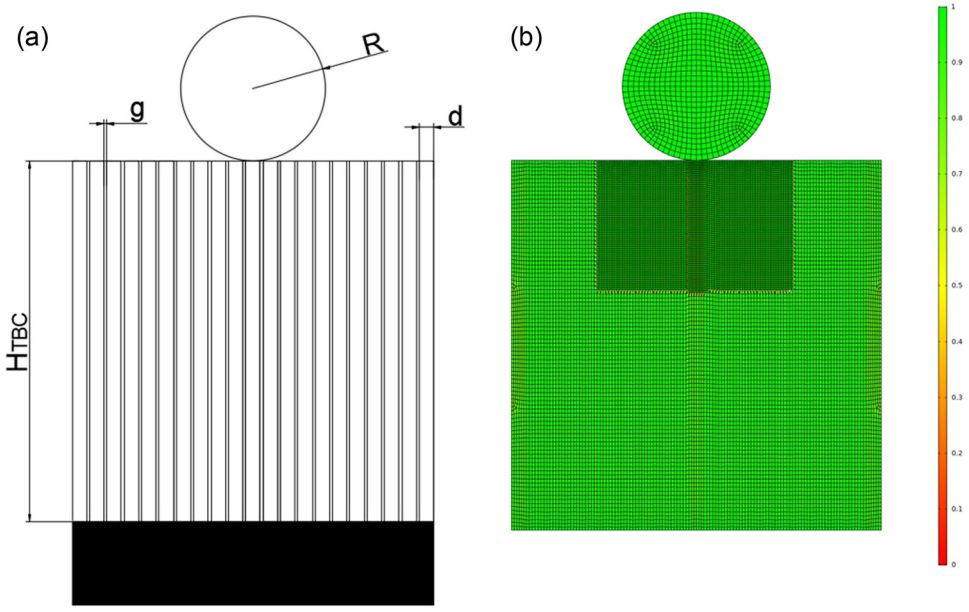

Figure 1: Finite element model and mesh generation of hard particle erosion coatings: (a) finite element model of hard particle erosion coating and (b) mesh generation of the finite element model.

Table 1: Relevant parameters of blade coating material [10]

Geometric parameters	Rectangular bar length H_{TBC} (μm)	Rectangular bar width d (μm)	Interstitial material g (μm)	Coating density ρTBC (kg/m^3)	Coating porosity f_o (%)
Value	100	5	0.1	5,900	10
Mechanical parameters	Young's modulus E_{TBC} (GPa)	Poisson's ratio v_{TBC}	Energy release rate G_{TBC} (J/m^2)	Fracture strength σ^c_{TBC} (MPa)	Yield strength σ^Y_{TBC} (MPA)
Value	40	0.12	20	287	150

When the maximum principal stress deviation fluctuates about 1% after the number of grids exceeds 26,000, we consider that the influence of the number of grids on the calculation accuracy can be neglected. Considering the computation time, it is reasonable to select the grid number of 26,000.

2.2 Finite element modeling of crack propagation

The simulation of crack growth in this section is mainly based on the classical fracture mechanics model and the damage fracture mechanic model [18]. The essential difference between the two models lies in the fracture conditions. For classical fracture mechanics model, the fracture occurs when the material undergoes a transformation from elastic to plastic deformation. Comparatively, the damage fracture mechanics model is based on the damage failure of the material, *i.e.*, the material would fracture when the material damage failure develops to a certain extent.

The simulation of crack propagation in pump components uses the initial fracture criterion as the maximum principal stress criterion, in which the critical maximum principal stress of the blade coating is 287 MPa, as shown in Table 1. Specifically, when the maximum principal stress is larger or equal to 287 MPa, the pump components would be damaged. The damage evolution criterion is a proportional weakening criterion with an energy release rate of 20 J/m^2. The constitutive relationship of this article is a model coupling linear elasticity with linear softening, as shown in Figure 2. In this figure, the vertical and horizontal axes represent the maximum principal stress and the deformation displacement δ of pump component material, respectively. During the material deformation of pump components, when the amount of deformation reaches δ^0, the pump component starts to have wearing problems and then evolves according to the curve 2–3–4. Moreover, when δ reaches position 4, a triangle forms and its area represents the energy loss rate. At this time, the energy release rate has just reached 20 J/m^2 where a complete damage of pump components occurs.

It should be noted that the process of 1–4 in Figure 1 is dynamic. Therefore, the dynamic analysis step (Dynamic Analysis Step) should be used in the finite element ANSYS simulation process, but the finite analysis method has certain limitations on dynamic analysis, such as only the implicit analysis step can be used. In this article, Dynamic Implicit Analysis Step is chosen.

Table 2: The result of grid independent verification

The number of grids	17,721	21,438	22,973	23,622	26,000	28,155	32,252
The maximum principal stress (MPa)	185.43	152.69	149.93	145.63	144.41	145.81	143.95
Deviation (%)	—	17.65	1.81	2.87	0.84	0.97	1.27

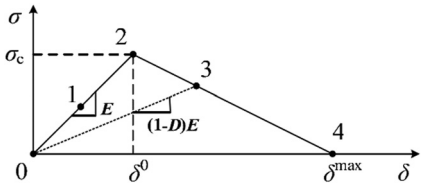

Figure 2: Linear elasticity–linear softening model.

3 Results and discussion

The flowing law in the shield pump is extremely complicated, and the angle, velocity, and trajectory of the hard particle in the pump vary when the hard particle impacts the flow passage components [19]. Therefore, it is of great significance to study the flowing law and the transportation trajectories of the hard particle in the shielded pump for grasping the blade loss.

3.1 Analysis of impact process

First of all, the hard particle impacts the blade manufactured by the material HAC276 (as a TBC, its performance parameters are shown in Table 1) at the initial velocity (v_0) of 80 m/s and angle of 90°, then the distribution diagrams of the maximum principal stress (σ_{max}) of the blade material at different time (0.079, 0.14, 0.2, and 0.3 ns) are shown in Figure 3. According to the maximum principal stress distribution diagram, it can be seen that, after the hard particle impacts the blade, a ring-shaped ripple forms at the contact position of the hard particle and the blade material before expanding to the inside of the blade material. At the first time point, *i.e.*, 0.079 ns, the area of maximum principal stress is distributed on both sides of the hard particle. Then this area spreads to the inner surface of the coating at the time point of 0.143 ns. It is noted that this area extension stops at the time point of 0.2 ns when it decreases gradually. This is because the hard particle begins to enter the rebound stage when the correspondingly maximum principal stress value also decreases. Finally, at the last time point 0.3 ns, the hard particle finishes rebound and the maximum principal stress returns to the normal value.

Figure 4 shows the variation of the support reaction with time exerting on the hard particle during the impacting of the blade material. It can be seen that the support reaction of the hard particle rises to the maximum value at 0.2 N in a very short period of time. Then, the support reaction begins to decline. At the time point of 0.1 ns, the support reaction almost drops to zero, which physically means that the hard particle and the blade material are completely separated.

According to the variation of support reaction with time in Figure 4, when the hard particle impacts the blade material, the acceleration first increases and then decreases. For the variation of displacement with time, it can be seen that the displacement has a peak at 0.051 ns, which indicates that the hard particle has reached the maximum value that the blade material can accept. The smaller displacement after reaching the peak indicates that the subsequent hard particle begins to rebound.

According to the variation of the support reaction and displacement, the hard particle enters the rebound process after 0.079 ns. The rebound process consists of three stages. The first stage is the period of 0.079–0.1 ns, during which the hard particle begins to contact and collide with the blade material, resulting in interaction forces. The second stage is the period of 0.1–0.2 ns, during which the hard particle starts to rebound but still contact and collide with blade material without interaction forces. The third stage happens after 0.2 ns, during which the hard particle does not contact and collide with the blade material without interaction forces. Therefore, the support reaction first rises and then decreases before reaching zero. The reasons for this are explained as below. Initially, the hard particle impacts the blade material with great energy, so the support reaction exerting on the hard particle will rise to the maximum value in a very short time. However, as time passes, the blade material begins to recover to its initial shape, the collision state begins to ease, and the supporting force begins to decline. Eventually, the hard particle completely rebound and does not contact the blade material without interaction force. Correspondingly, the support reaction drops to zero.

Figure 5 shows the displacement variation of the hard particle with time during the collision. It can be seen from Figure 5 that the displacement area of blade

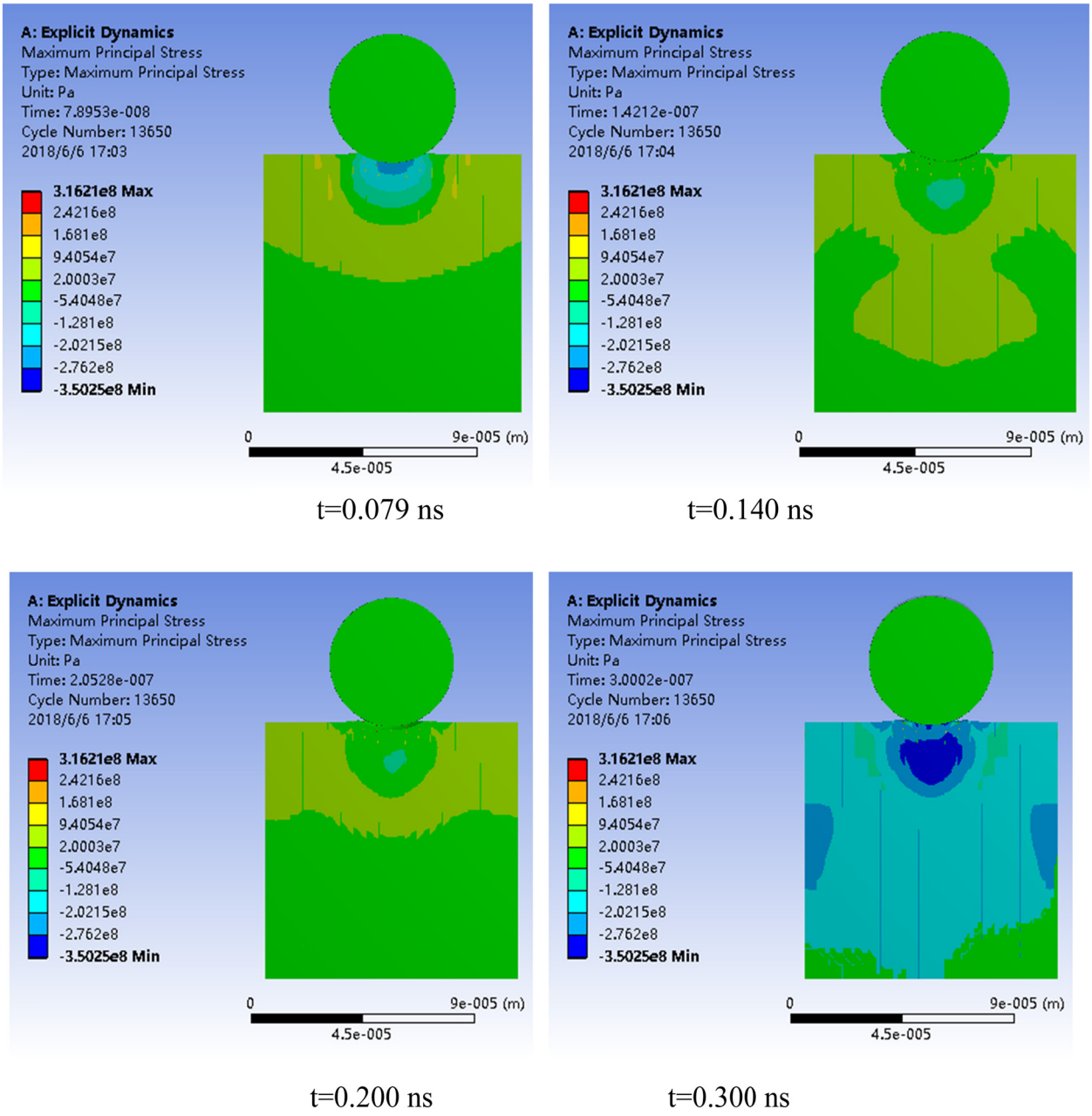

Figure 3: Simulated maximum principal stress σ_{max} contour at different time.

material is largest at 0.079 ns during the movement of the hard particle. This is because the hard particle exerts the maximum force on the blade material at this time. As time increases, the displacement area gradually decreases. The maximum contact displacement appears on the contact surface where the particles impact the TBC system, and damage or even cracks occur at the TBC contact position.

Combining our simulation with Hertz's contact theory, the impacting process of ball-end on coatings can be divided into two stages. The first stage is the ball impacts the coating surface. When the relative impact velocity is 0, the compression deformation of material surface reaches the maximum value. In the second stage, after the elastic deformation of the material, the ball-end is given an impulse, resulting in a crown damage indentation on the surface of the material and twice rebounds of the ball. Moreover, there are bumps around the indentation, many wide radial cracks outside of the indentation, and also a few circumferential cracks with different concentric radii inside of the indentation. As shown in Figure 6, it is found that in the actual production process, the G1-512 shield pump [21] experiences a sharp drop in fluid supply

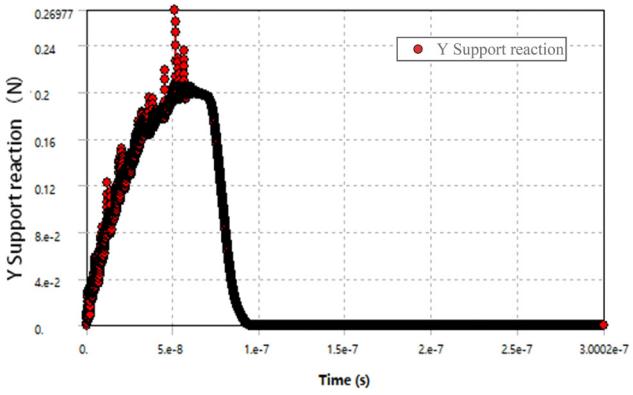

Figure 4: Time-dependent curve of the support reaction of the hard particle during the erosion process (The red dots represent the support reaction, and the black lines are the display problems caused by too many red dots.).

and a sharp increase in flutter. After disassembling the pump, it is found that the impeller is lost and damaged under the impact of the fluid. So the dimensional accuracy of flow passage components is reduced. The above-mentioned impacting process of the hard particle on pump parts can be well simulated by finite element method, which verifies the established model.

3.2 Effect of impact velocity on erosion process

In this section, the effect of collision velocity of hard particle on the maximum principal stress is investigated

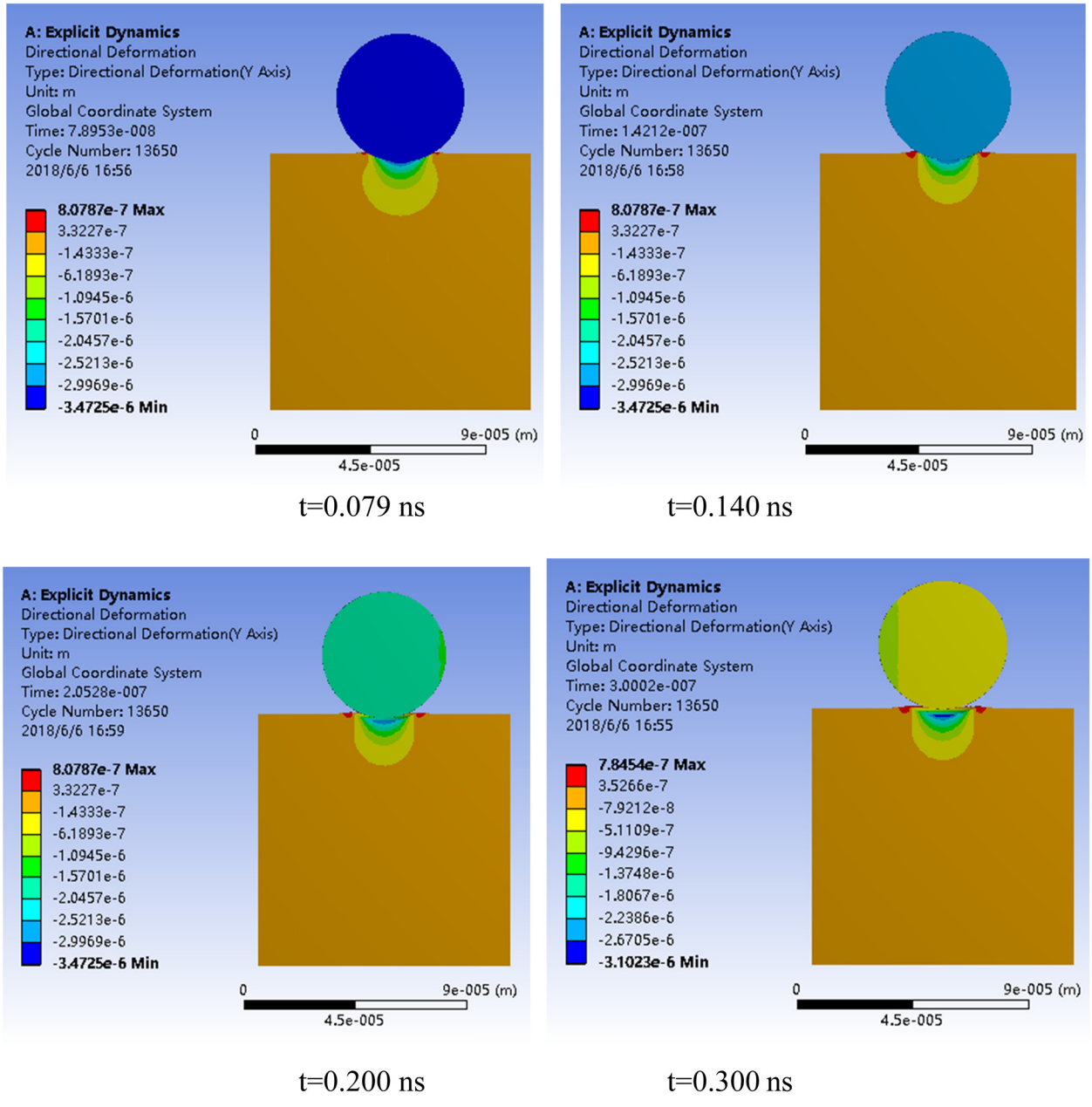

Figure 5: Displacement variation of hard particle with time during erosion.

(a) (b)

Figure 6: Failure of the shield pump [20]: (a) flow passage component and (b) impeller maintenance status.

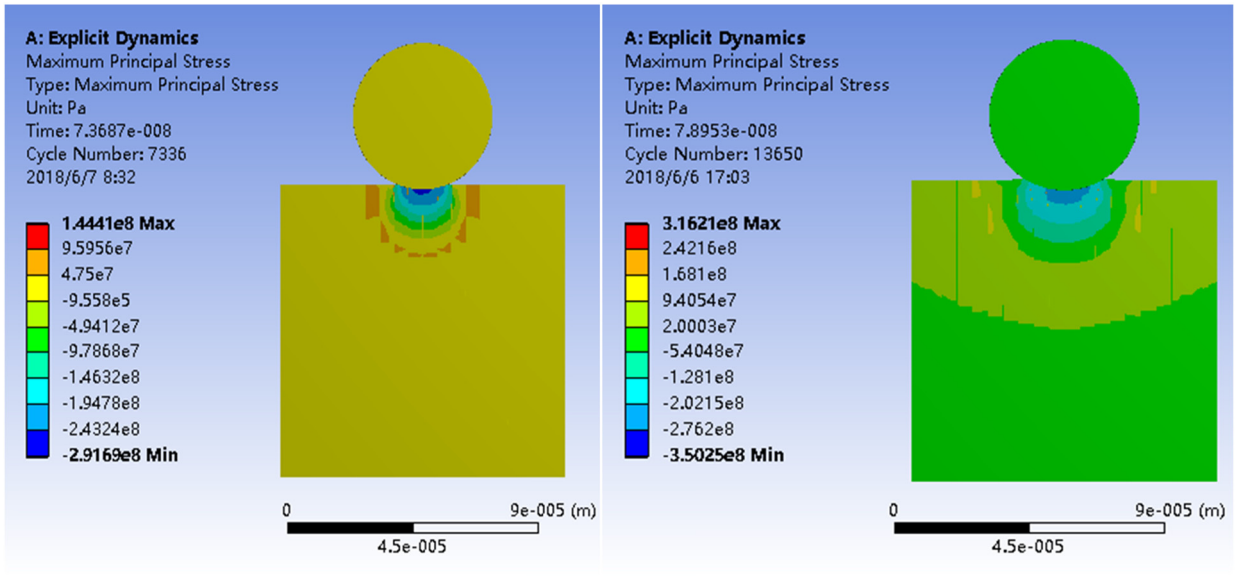

v_0=40 m·s^{-1} v_0=80 m·s^{-1}

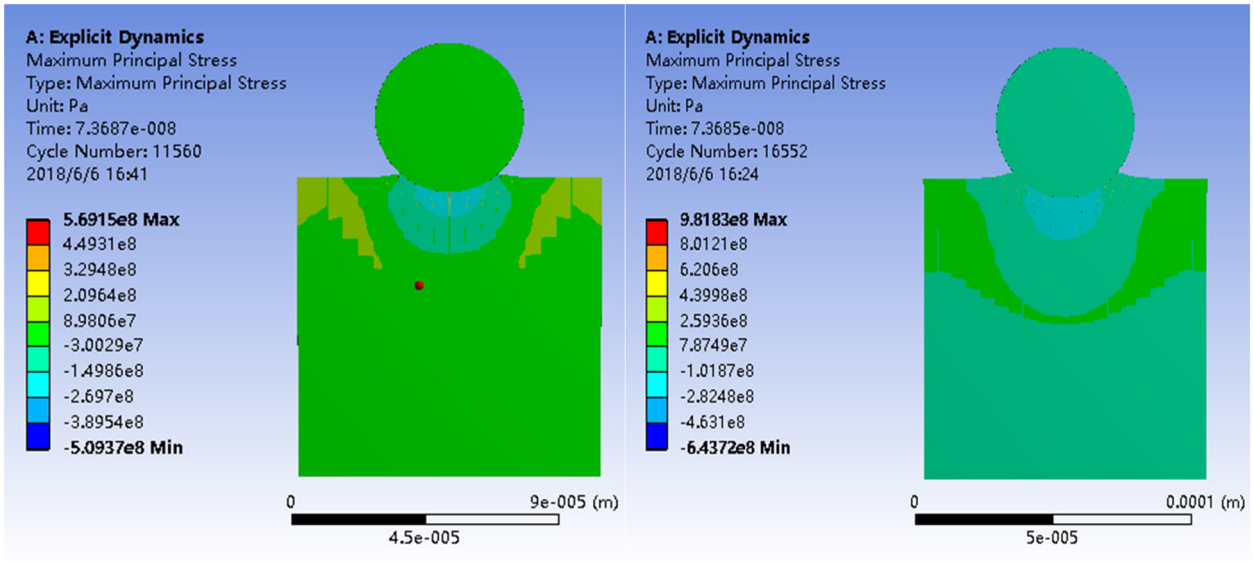

v_0=120 m·s^{-1} v_0=160 m·s

Figure 7: Maximum principal stress nephogram at different collision velocities.

with initial velocities at 40, 80, 120, and 160 m/s, as shown in Figure 7. When the particles impact the TBC system at different initial speeds, it can be clearly seen that the maximum principal stress increases rapidly with the increase of velocity. The maximum principal stress is 144 MPa when the impact velocity of the hard particle is 40 m/s, compared to 982 MPa at a velocity of 160 m/s. The maximum principal stress appears in the collision contact area between the hard particle and the coating. With the increase of time, the particle-coating collision deepens, and the maximum principal stress appears below the collision area and moves to both sides of the coating gradually. Meanwhile, with the increase of the initial velocity of the hard particle, the kinetic energy of the hard particle increases. Therefore, more energy is transformed into the deformation of the blade material, which is reflected by a deeper pit after the hard particle impacts the blade material.

Furthermore, the relationship between the maximum principal stress and the direction deformation of the blade with time under different impact velocities is given, as shown in Figures 8 and 9. In Figure 8, we use the ratio of maximum principal stress to yield stress as the ordinate. It can be seen that the internal stress of the blade will gradually disappear after the impact of hard particles at a lower impact velocity of 40 m/s. However, with the increase of impact velocity, especially at 160 m/s, the second wave-crest stress will be generated in the blade material after impact, which may be the main factor leading to blade failure. Figure 9 shows the internal deformation of the blade, and its ordinate is dimensionless by the ratio of the maximum displacement to the

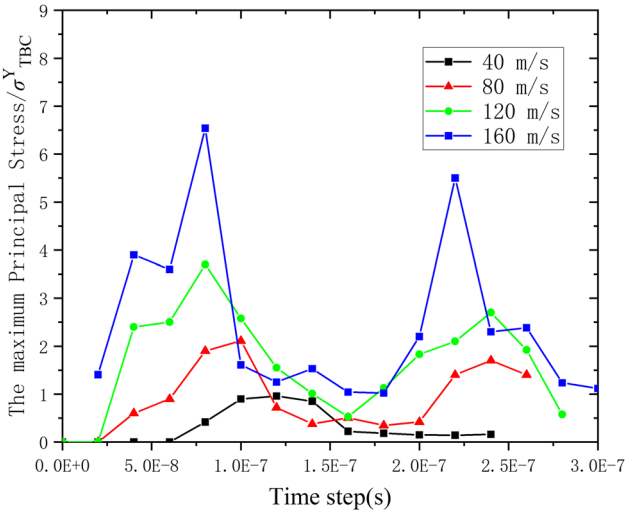

Figure 8: Relationship between maximum principal stress and time step in blade under different impact velocities.

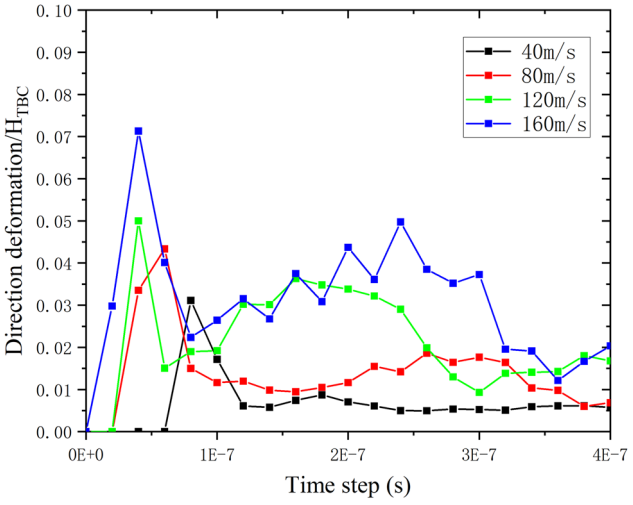

Figure 9: Relationship between direction deformation and time step in blade under different impact velocities.

total height of the blade. At a lower velocity of 40 m/s, the deformation of the blade will recover soon after the collision. And as the velocity increases to 160 m/s, the internal deformation of the blade will rebound after the particles leave the blade, but it remains at a large value with time, and is difficult to recover, which ultimately leads to the formation of pits.

From the above analysis, it can be seen that the impact velocity of the particles will significantly affect the service life of the blade. This explains the phenomenon that the impeller edges, upper and lower surfaces are easy to wear in the actual production. Therefore, reasonable selections of the blade velocity are of significance for eliminating blade erosion. In other words, the wear resistance of flow passage parts can be ensured and their service life can be extended by avoiding utilizing high speeds.

3.3 Effect of impact angle on erosion process

One of the most important characteristics of impact wear is that the erosion rate varies with the impact angle. Therefore, studying the effect of the impact angle of the hard particle on the erosion wear rate is significant for understanding the wearing mechanisms of blades. The impeller of the shielded pump is made of metal materials. The relationship between the erosion wear rate and the impact angle is shown in Figure 10. It can be clearly seen that there are two peaks on the curve. Specifically, the erosion wear rate increases with the increase of impact

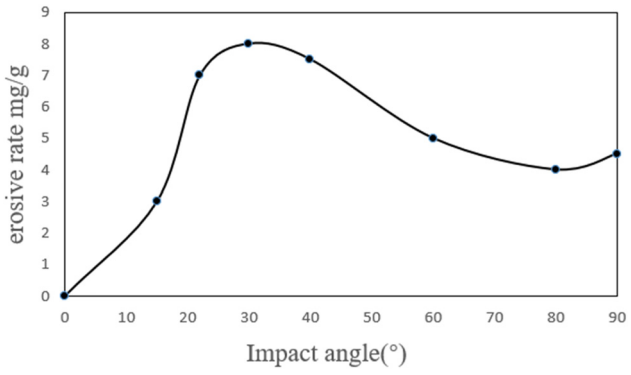

Figure 10: Effect of impact angle on erosion rate of coating.

angle and reaches the first peak at an impact angle of 30°. Then the erosion wear rate decreases with the increase of impact angle and reaches the second peak at an impact angle of 90°. Considering the distinctiveness of the two peaks, the impact of the hard particle at angles of 30° and 90° are simulated and the corresponding effect of impacting angle on the impellers is compared.

Figure 11 shows the maximum principal stress distribution at impacting angles of 30° and 90°, and the impact velocity of 120 m/s. The maximum principal stress varies from 800 to 500 MPa as the impact angle increases from 30° to 90°, which confirms the variation law demonstrated in Figure 10. As can be seen from Figure 11, the impact position and angle affect both the distribution and magnitude of maximum principal stress. Moreover, the peak principal stress appears to the left of the hard particle at 30°, while the maximum principal stress distribution is symmetrical at 90°. Previous studies have shown that the cutting damage is dominated on the

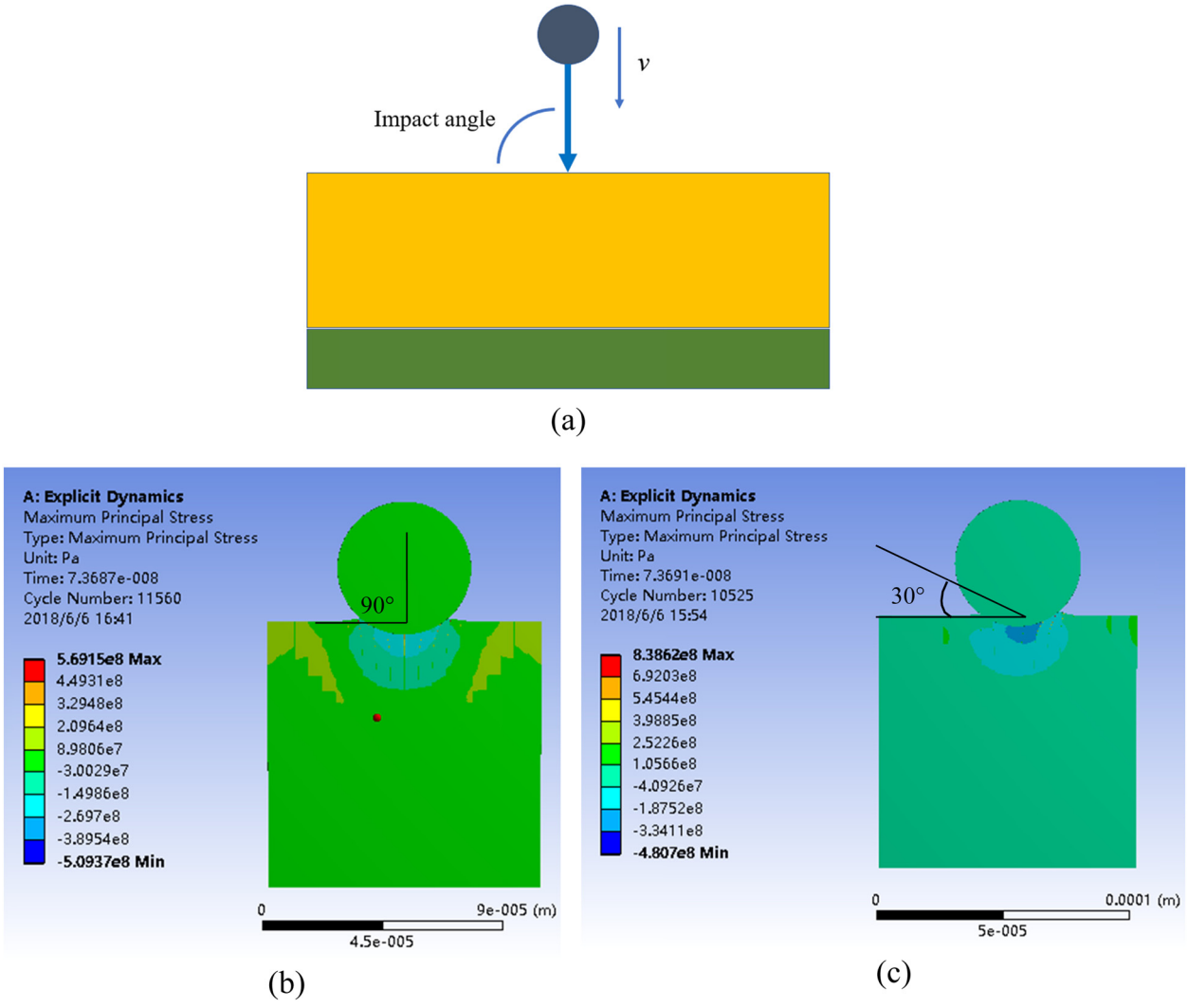

Figure 11: Schematic diagram and contour: (a) schematic diagram of particle impact angle, (b) maximum principal stress contour at an impact angle of 90°, and (c) maximum principal stress contour at an impact angle of 30°.

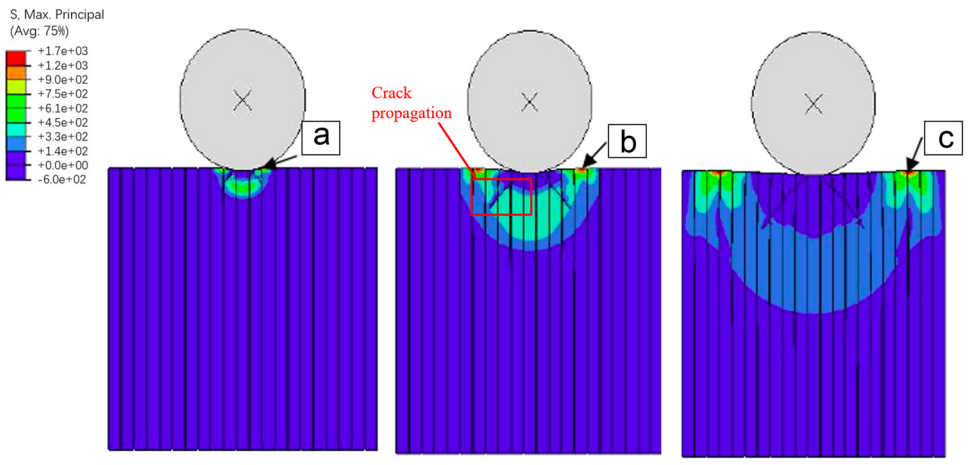

Figure 12: The maximum principal stress σ_{max} contour of the crack propagation at a specific moment: (a) maximum principal stress at region A during crack initiation, (b) maximum principal stress at region B during crack propagation, and (c) maximum principal stress at region C during crack propagation into the impeller.

material surface under low-angle erosion, and results in lip turning, plowing, *etc*. However, the erosion pit damage is dominated on the material surface under high-angle erosion [22]. When the hard particle impacts the blade material, the maximum deformation of the blade material decreases with the increase of the impact angle. It can be seen that the velocity of the hard particle can be divided into the horizontal velocity and the vertical velocity under different impact angles. The two velocities result in the horizontal force and vertical force acting on the coating. The vertical force mainly leads to the extrusion effect on the material and further erosion pits, while the horizontal force mainly results in cutting effect to remove the surface material. In conclusion, in the process of erosion, horizontal cutting and vertical extrusion coexist, but the wear rate at 30° is significantly higher than that at 90°, which indicates that the erosion damage of the blade material is mainly due to the cutting. This explains the phenomenon that the impeller corners of the inlet and outlet are easy to wear in the actual production and provides theoretical guidance for the geometric design of the shielded pump. Therefore, the impacting angle of 30° should be avoided in the design and employment of the pump.

3.4 Analysis of erosion crack propagation

When the blade material is subjected to certain stress and deformed by the impact of the hard particle, the surface of the blade begins to initiate microcracks. With the continuous impact of the hard particle, the impeller crack begins to expand before a continuous propagation, finally the material removal phenomenon even appears on the blade surface. Therefore, the study on the crack initiation and propagation on the surface of impacted blade is important for understanding the failure mechanism and optimizing the performance of the blade. The hard particle with a radius of 25 μm impacts the blade material vertically at an initial velocity of 180 m/s in the simulation. The simulation results are shown in Figure 12, which demonstrate the process from crack initiation to propagation. It can be seen from Figure 12(b) that the crack expands at 45° from the horizontal axis.

From the crack propagation in Figure 12, it can be seen that the local plastic deformation occurs near the collision surface between the hard particle and the impeller with the applied load. The increased load causes an increased collision opening angle which expands in a direction of 45° from the surface of the blade, and the propagation path passes through parts with different materials and continuously expands. Moreover, the variation of stress distribution around the collision point is shown in Figure 9. The area of maximum principal stress at the collision point, with a peak at 1,200 MPa, is distributed symmetrically in the shape of a butterfly along the *y*-axis. As the collision process continues, the maximum stress expands from region A to region C. In this process, the collision area has experienced plastic deformation and crack propagation. The maximum principal stress decreases in a fan shape from the hard particle collision point to the surrounding area, and the rest of the area is almost in a state of zero stress. In Figure 12(b), it can be seen that the stress value in the area around the crack reaches 450 MPa, which exceeds the yield strength of the material, indicating that plastic deformation has occurred in this area and the crack has

expanded forward as shown in Figure 12(c). The aforementioned simulated findings regarding stress variation and material removal provide a specific data basis for the selection and processing of impeller materials in actual production, contributing to reducing the fracture rate of the impeller.

4 Conclusion

In this article, the structural static analysis module is used to simulate the erosion process in shield pump flow passage by hard particle. Then the variation law of stress, strain, and material deformation of the flow passage components under concentrated force is obtained. Second, an elastic–linear softening model is established, and the finite element modeling of crack propagation is performed by using the dynamic implicit analysis step. Then the stress variation during the crack propagation and material removal under the continuous erosion by hard particle is obtained.

The specific conclusions are as follows:

1) In the impact–rebound–disengagement process of the hard particle, a ring-shaped ripple forms at the contact position after the hard particle impacts the blade and then expands to the inside of the blade material. This means the area of maximum stress diffuses to the inner surface of the coating. The impact load generated by the hard particle is largest at the time point of 0.051 ns. Correspondingly, the blade stress is concentrated in the area right below the impacting center and reaches its maximum value. At the time point of 0.1 ns, the hard particle and the coating are completely separated. Meanwhile, the internal stress of the blade spreads to both sides, and the stress value decreases. The above process agrees well with Hertz contact theory, which verifies the established model.
2) The impact velocity and angle of the hard particle affect the erosion process. The erosion velocity of particles significantly affects the service life of the blade. The higher the initial speed of the hard particle, the deeper the pit left by the impact of the hard particle on the blade material. In addition, the maximum deformation of the blade material decreases with the increase of the impact angle. The maximum erosion wear rate occurs at an impact angle of 30°. This can be used to explain the phenomenon that the impeller edges, upper and lower surfaces, and the corners of the inlet and outlet are easy to wear in the actual production. It also provides theoretical guidance for the selection of the specific working parameters and geometric design of the shielded pump.
3) By analyzing the crack propagation process, it is found that the maximum principal stress decreases in a fan shape from the hard particle collision point to the surrounding area. When the stress at the impact point reaches 1,200 MPa, local plastic deformation occurs, which further leads to crack propagation, while the internal stress of the impeller is maintained at 450 MPa. This finding provides a specific data basis for the selection and processing of impeller materials in actual production, contributing to reducing the fracture rate of the impeller.

Funding information: This work was supported by the National Natural Science Foundation of China (NSFC) – Shandong Joint Fund (U2006221), Shandong provincial fund (ZR2021ME161), Ocean industry leading talent team of Yantai's "Double Hundred Plan," Fundamental Research Funds of Shandong University (No. 2019HW041), and Key Laboratory of High-efficiency and Clean Mechanical Manufacture at Shandong University, Ministry of Education. The authors feel grateful for their kind support.

Author contributions: All authors have accepted responsibility for the entire content of this manuscript and approved its submission.

Conflict of interest: The authors state no conflict of interest.

References

[1] Wang L. Study on the performance of high-efficiency canned motor pump [dissertation]. Zhenjiang, Jiangsu: Jiangsu University; 2010.
[2] Kang H. Research on wear mechanism of centrifugal slurry pump [dissertation]. Xi'an, Shaanxi: Xi'an University of Architecture and Technology; 1999.
[3] Wu B. Study on solid–liquid two-phase three-dimensional turbulence and erosion wear characteristics of slurry pump [dissertation]. Changsha, Hunan: Central South University; 2010.
[4] Li W. Wear mechanism and finite element simulation analysis of centrifugal slurry pump [dissertation]. Xi'an, Shaanxi: Xi'an University of Science and Technology; 2007.
[5] Liu J. Improving the service life of slurry pump design. Gen Mach. 2006;4:86–8. doi: 10.3969/j.issn.1671-7139.2006.04.034.
[6] Finnie IJW. Erosion of surfaces by solid particles. Wear. 1960;3(2):87–103. doi: 10.1016/0043-1648(60)90055-7.

[7] Walker CI, Wells PJ, Bodkin GC. The effect of flow rate and solid particle size on the wear of centrifugal slurry pumps. 1994 American Society of Mechanical Engineers (ASME) Fluids Engineering Division summer meeting, Lake Tahoe, United States: N; 1994. p. 263.
[8] Yimin G, Jiandong X, Xin X. Study on erosion and abrasion characteristics of epoxy wear resistant adhesive coatings. J Xi'an Jiaotong Univ. 2001;3:319–21. doi: 10.3321/j.issn:0253-987X.2001.03.023.
[9] Kai G. Study on wear law of slurry pump impeller and ceramic coating protection [dissertation]. Kunming, Yunnan: Kunming University of Science and Technology; 2018.
[10] Lihua F. Finite element simulation of erosion process and crack propagation of EB-PVD thermal barrier coatings [dissertation]. Xiangtan, Hunan: Xiangtan University; 2013.
[11] Lei GU, Fusheng NI, Liqun XU. Experimental study on movement of particles in centrifugal impeller. J Drain Irrig Mach Eng. 2018;36(3):191–6.
[12] Xiuyun Z, Rong P, Yan L. Finite element analysis of impact test of steel plate concrete wall based on ANSYS/LS-DYNA. Explos Shock Waves. 2015;35(2):222–8. doi: 10.11883/1001-1455(2015)02-0222-07.
[13] Honghong H, Minxia Z, Tieshun J. Theoretical and finite element analysis of mechanical behavior of steel structure coatings impacted by sand particles. Chin J Appl Mech. 2014;31(06):830–5. doi: 10.11776/cjam.31.06.B121.
[14] Zhenzhu M, Hanwei Y, Yiwang B. Characteristics of contact damage morphology of rock and concrete after particle impact. J Yanshan Univ. 2009;33(6):510–6. doi: 10.3969/j.issn.1007-791X.2009.06.007.
[15] Li H. Prediction of impact abrasion at the bend of three-phase flow pipeline [dissertation]. Daqing, Heilongjiang: Northeast Petroleum University; 2013.
[16] Zhongdong Q, Yi W, Yuanyong Y. Numerical simulation of sand and abrasion of impeller of double suction centrifugal pump. J Hydroelectric Eng. 2012;31(3):223–9.
[17] Shen J. Simulation of steady and non-constant value of flow field in slurry pump [dissertation]. Lanzhou, Gansu: Lanzhou University of Technology; 2009.
[18] Wancheng Z, Chunan T, Qilin Z. Mechanical model and numerical simulation of concrete fracture process. Prog Mech. 2002;4:579–98. doi: 10.6052/1000-0992-2002-4-J2001-001.
[19] Jiutai C, Hongbo W, Guangyun G. Optimization of the wrap angle of the cylindrical blade of centrifugal slurry pump. Fluid Machinery. 2005;3:34–6. doi: 10.3969/j.issn.1005-0329.2005.03.010.
[20] Tian X. Research on impact damage and finite element simulation of steel structure coatings under impact loads [dissertation]. Hohhot, Inner Mongolia: Inner Mongolia University of Technology; 2019.
[21] Li L. Failure analysis and modification of slurry pump in PTA unit. Gen Mach. 2014(6):66–7.
[22] Zhiguo W, Yihua D, Junsheng L. Experimental study on the impact of impact angle and injection velocity on erosion rate of super 13Cr tubing. J Xi'an Shi you Univ (Nat Sci Ed). 2016;31(5):100–5.